Hydrogen Stretching Vibrational Circular Dichroism in Methyl Lactate and Related Molecules

Denise M. P. Gigante,† Fujin Long, Louise A. Bodack, Jeffrey M. Evans,‡ James Kallmerten, Laurence A. Nafie,* and Teresa B. Freedman*

Department of Chemistry, Syracuse University, Syracuse, New York 13244-4100

Received: September 21, 1998; In Final Form: January 7, 1999

The CH- and OH-stretching vibrational circular dichroism (VCD) spectra of methyl lactate and related molecules in CCl_4 solution have been investigated to identify solution conformations and establish a correlation between OH- and methine-stretching VCD intensity and molecular structure. Deuterium substitution was used when possible to remove overlapping absorption features in the CH-stretching region. Anisotropy ratios between $+2.1 \times 10^{-4}$ and $+2.8 \times 10^{-4}$ were measured for the methine-stretching VCD of the molecules with both α-oxy and α-C═O substituents: (*S*)-methyl-d_3 lactate, (*S*)-methyl-d_3 2-(methoxy-d_3)-propionate, di(methyl-d_3) D-tartrate, (*S*)-methyl-d_3 mandelate, (*S*)-methyl-d_3 *O*-(acetyl-d_3)-mandelate, and (*S*)-benzoin. The methine-stretching VCD intensity serves as a marker for both absolute configuration and solution conformation in these molecules, as previously demonstrated for amino acids and peptides. In (*S*)-methyl 2-chloropropionate, (*R*)-methyl 3-hydroxy-2-methylpropionate, and (*S*)-methyl 3-hydroxybutyrate, the net CH-stretching VCD intensity is small relative to that in the other molecules studied. Ab initio calculations of geometries, vibrational frequencies, and unpolarized infrared absorption (IR) and VCD intensities were carried out to identify the most abundant solution conformers from the VCD spectra and to correlate OH- and methine-stretching VCD intensity with molecular conformations. Factors leading to large methine-stretching VCD anisotropy ratios are assessed.

Introduction

Vibrational circular dichroism (VCD),[1−3] the differential absorbance of left and right circularly polarized infrared radiation during vibrational excitation of a chiral molecule, provides a sensitive probe of absolute configuration and solution conformation. The fast time scale of vibrational spectra allows observation of molecular conformations that interconvert on an NMR time scale. Hydrogen stretches are largely decoupled from lower energy vibrational motion in molecules, and can occur as highly localized group modes. As such, hydrogen stretches in chiral molecules are particularly well suited as markers for molecular configuration and conformation through their VCD intensity.[4] VCD spectra in the NH- and OH-stretching regions have been used to identify solution conformations in ephedra drugs,[5] propranolol,[6] and tripodal peptides.[7] The methine-stretching VCD often serves as a marker for the absolute configuration of a chiral carbon center, as demonstrated for amino acids and peptides.[8,9] The methine-stretching mode can generate some of the largest VCD signals that have been observed for an isolated vibrational motion,[4,10−12] with anisotropy ratios ($\Delta A/A$) on the order of $1-3 \times 10^{-4}$. In contrast to the conservative VCD spectra that arise from the coupling of chirally oriented local oscillators (integrated intensity that sums to zero over the region of coupling), the methine stretch imparts a large bias to positive or negative intensity in the CH-stretching VCD spectrum for several types of chiral environments of the methine CH bond. The intense monosignate methine-stretching VCD signal persists when vibrational coupling is minimized by deuterium substitution of neighboring CH bonds.[13] The mechanism that gives rise to this large VCD signal for an uncoupled methine stretch is not yet fully understood. An early empirical descriptive model for the explanation of these large VCD signals was the ring current mechanism, proposed by Nafie, Freedman, and co-workers,[4,14−16] in which the contraction or elongation of a single oscillator adjacent to certain types of intramolecular rings closed by transition-metal coordination or hydrogen-bonding was proposed to generate an oscillating electronic current around the ring that gives rise to a magnetic dipole transition moment perpendicular to the ring plane. A set of empirical rules was developed to predict the sense of electronic charge circulation about the ring, depending on the relative orientations of the ring and methine bond, wherein strong VCD intensity was predicted to be generated by an oscillator oriented perpendicular to the ring and weak VCD for an oscillator lying in the plane of the ring.[4] However, this empirical model was criticized on the basis of the results of ab initio calculations of VCD intensity on hydrogen-bonded and non-hydrogen-bonded conformations of (*R*)-methyl lactate-d_6[17] and (*R*)-methyl glycolate-d_1.[18] The methine-stretching VCD feature was calculated to be large whether or not a hydrogen-bonded ring was present. This result implies that the formation of vibrationally generated electronic ring currents through bonds is likely not responsible for the large methine-stretching VCD intensities, thus calling into question the premise of the ring current model. With the more widespread application of ab initio VCD intensity calculations,[3,19−21] the focus of the interpretation of VCD spectra has generally shifted from the consideration of

* Authors to whom correspondence should be addressed. Fax: (315) 443-4070. E-mail: tbfreedm@syr.edu; lnafie@syr.edu.

† Current address: Department of Chemistry, Onondaga Community College, Syracuse, NY.

‡ Current address: Bristol Myers Squibb Co., Syracuse, NY.

10.1021/jp9837885 CCC: $18.00
Published on Web 03/02/1999

SCHEME 1

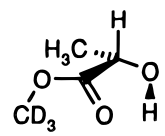

(*S*)-methyl-d_3 lactate
(I)

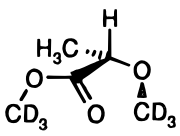

(*S*)-methyl-d_3 2-(methoxy-d_3)-propionate
(II)

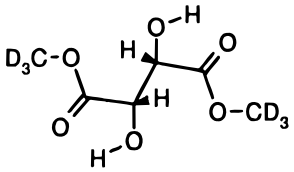

di(methyl-d_3) D-tartrate
(III)

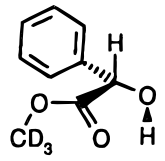

(*S*)-methyl-d_3 mandelate
(IV)

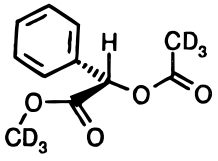

(*S*)-methyl-d_3 *O*-(acetyl-d_3)-mandelate
(V)

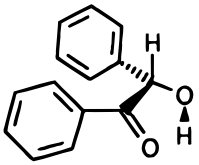

(*S*)-benzoin
(VI)

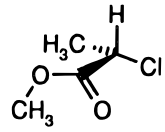

(*S*)-methyl 2-chloropropionate
(VII)

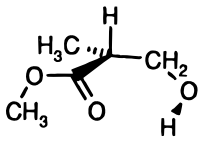

(*R*)-methyl 3-hydroxy-2-methylpropionate
(VIII)

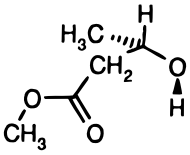

(*S*)-methyl 3-hydroxybutyrate
(IX)

mechanistic models for the VCD intensity of individual vibrations to comparisons of the overall VCD intensity pattern calculated for a conformer or set of conformers with the observed VCD spectrum.

We have recently renewed our interest in the mechanisms of VCD intensity through our development of calculations of vibrational transition current density (TCD).[22−24] TCD plots allow the visualization of the flow of electrons caused by nuclear motion. The observation of vibrationally generated circulatory electronic motion about atomic centers, as well as angular motion across groups of nuclei, in TCD calculations for nonchiral molecules,[24] reopens the question of whether regular patterns of electronic motion in chiral molecules exist that can be associated with the magnetic dipole moment content of VCD intensity.

As a basis for correlating the results of TCD calculations with experimental VCD measurements, the present investigation provides empirical evidence for the effect of adjacent hydrogen-bonded and non-hydrogen-bonded groups on the methine-stretching VCD intensity. In addition, we seek to establish the applicability of sum-over-states vibronic coupling theory (VCT) calculations of VCD intensity[25−27] in the CH- and OH-stretching regions, since our implementation of vibrational TCD involves similar sum-over-states computations.[24] Finally, this study further characterizes the chiral environments leading to intense methine-stretching and OH-stretching VCD for use as markers for absolute configuration and conformation in larger molecules containing similar groups, and demonstrates the utility of VCD in identifying the most abundant solution conformers in this class of molecules.

In this investigation, the CH- and OH-stretching VCD spectra of a variety of hydroxy esters and other molecules related to methyl lactate are reported. Deuterium substitution has been incorporated for several of the molecules to remove overlapping absorption features, to make accurate measurements of methine-stretching anisotropy ratios. To elucidate the molecular environments that generate large methine stretching VCD, the groups adjacent to the methine have been varied, including substitutions that retain the local chiral environment of the methine bond, but which prohibit hydrogen bonding.

The structures of the nine molecules studied, (*S*)-methyl-d_3 lactate (**I**), (*S*)-methyl-d_3 2-(methoxy-d_3)-propionate (**II**), di-(methyl-d_3) D-tartrate (**III**), (*S*)-methyl-d_3 mandelate (**IV**), (*S*)-methyl-d_3 *O*-(acetyl-d_3)-mandelate (**V**), (*S*)-benzoin (**VI**), (*S*)-methyl 2-chloropropionate (**VII**), (*R*)-methyl 3-hydroxy-2-methylpropionate (**VIII**), and (*S*)-methyl 3-hydroxybutyrate (**IX**), are shown in Scheme 1. For several of these molecules, OH- and/or CH-stretching VCD spectra have been previously reported for the nondeuterated species.[4,28−30] The methine-stretching VCD of tartaric acid[28] and lactic acid in D_2O have also been reported.[8]

Experimental Section

The R- and S-enantiomers of methyl 2-chloropropionate (**VII**), methyl 3-hydroxy-2-methylpropionate (**VIII**), methyl 3-hydroxybutyrate (**IX**), methyl lactate, dimethyl tartrate, and methyl mandelate, and the S enantiomer and racemic mixture of benzoin (**VI**) were purchased from Aldrich and were used without further purification. Syntheses of the deuterium-substituted molecules, **I**−**V**, were carried out by the synthetic procedures recorded in the Appendix.

Spectra were recorded in the CH-stretching region for samples at 0.005 or 0.01 M concentration in CCl_4 solution, in a 1.0 cm

SCHEME 2

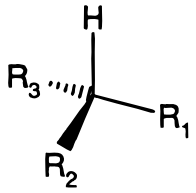

fixed path length cell equipped with CaF_2 windows. The solvent, spectrophotometric grade CCl_4, was purchased from Aldrich and dried over molecular sieves before use. Spectra in the OH-stretching regions of **I**, **VI**, **VIII**, and methyl lactate were obtained under these same conditions.

Infrared (IR) spectra were measured on a Midac Fourier transform infrared (FTIR) instrument with a resolution of 4 cm^{-1}, or for **VI** on a Bruker FS55 Step-Scan FTIR at 16 cm^{-1} resolution. Fourier deconvolution, baseline adjustment, and curve fitting were obtained by using SpectraCalc or Grams32 software (Galactic Industries Corp., Salem, NH). VCD spectra were recorded at 14−16 cm^{-1} resolution using a dispersive instrument,[31−34] with two to four scans averaged for each enantiomer, or (for **VI** and the OH-stretching region of methyl lactate) on a Bruker IFS55 FTIR−VCD spectrometer in step-scan mode, 2−4 h collection per sample, 16 cm^{-1} resolution.[35] The VCD baseline artifacts were eliminated by recording one-half the difference between the raw VCD spectra of the S and R enantiomers, with the exception of benzoin, for which a racemic sample was used for the baseline adjustment.

In addition to the hydrogen stretching spectra, the VCD and IR spectra of (*S*)-methyl lactate were obtained in the 1000−1600 cm^{-1} region for a sample 0.2 M in CCl_4 solution, 100 μm path length, 4.0 cm^{-1} resolution, on a Nicolet Magna 850 FTIR−VCD instrument, in simultaneous rapid-scan mode.[36]

Calculations of optimized geometries and vibrational frequencies for stable conformers of **I**, **II**, **VII**, **VIII**, and **IX** were carried out with Gaussian 94,[37] utilizing both density functional theory (DFT/B3LYP) and Hartree−Fock methods. The basis set 6-31G$^{(0.3)}$, based on 6-31G(d) with the d-orbital exponent reduced from 0.8 to 0.3, was employed for both these and the subsequent sum-over-states vibronic coupling theory (VCT) calculations of VCD intensity.[26,27,38] The latter calculations were carried out with the program VCT94, our adaptation of the original VCT90 program of Rauk and co-workers[26] to utilize Gaussian 94 output and parameters. For these VCT calculations, the modified 6-31G$^{(0.3)}$ basis set has been shown to yield calculated VCD intensities in good agreement with experiment.[20,38,39] Geometry and vibrational frequency calculations were also carried out previously with Gaussian 90[40] at the HF level (6-31G(d) basis for **I**, **II**, and **VII** and 3-21G basis for **IV**, **V**, and **VI**) to identify stable conformers, and compare relative energies and vibrational frequencies.[41]

Results

The series of nine molecules, **I**−**IX**, compared here have the general form C*$HR_1R_2R_3$, with chiral orientation as defined in Scheme 2. All contain a carbonyl group in an ester, deuterated ester, or ketone in the R_2 position, except for **IX**, in which a methylene is inserted between the methine and the ester group. The R_1 position, except for **VIII** which is $-CH_2OH$, is occupied by a heteroatom, in a methoxy, *O*-acetyl, hydroxy, or chloro group. A phenyl or a methyl group is in the R_3 position, except for **III**. A comparison of the CH-stretching absorbance and VCD spectra of the R enantiomers of di(methyl-d_3) tartrate (**III**) and methyl 3-hydroxy-2-methylpropionate (**VIII**) and the S enantiomers of the other seven molecules are presented in Figures 1 − 3. The molecules have been grouped by similar functional groups, and the absorbance or VCD spectra are displayed on the same ordinate scale, molar absorptivity (ϵ) or $\Delta\epsilon \times 10^3$, respectively, with the exception of the absorption spectra of **VII**−**IX**, for which a larger molar absorptivity range was required since these molecules were not deuterated. All nine molecules have a corresponding chiral arrangement of groups about the methine, even if the absolute configuration designation is not the same. The CH-stretching frequencies, intensities, and assignments for molecules **I**−**IX** are listed in Table 1. The experimental values of the frequencies, intensities, and anisotropy ratios for the methine-stretching modes (as assigned below) are presented in Table 2. The anisotropy ratios were calculated using integrated peak areas for both VCD and IR bands. Since the resolution of the absorbance and VCD spectra differs for some of the samples, the areas were obtained from optimal curve fits, taking into account the possible Fermi resonance components for the symmetric methyl-stretching modes when necessary.[13,42] The OH-stretching VCD and absorbance spectra assignments for (*S*)-methyl lactate,[30] dimethyl D-tartrate,[43] (*S*)-methyl mandelate (**IV**),[4,44] (*S*)-benzoin (**VI**), (*S*)-methyl 3-hydroxy-2-methylpropionate (**VIII**), and (*S*)-methyl 3-hydroxybutyrate (**IX**)[30] are also listed in Table 1. These measurements are presented for the parent, nondeuterated species.

The calculated structures and relative energies of selected stable conformers of **I**, **II**, **VII**, **VIII**, and **IX** are depicted in Figures 4 and 5. Calculated VCD spectra for these conformers are compared with experimental data in Figures 6−16, and calculated structural data, methine- and OH-stretching frequencies and anisotropy ratios are compiled in Tables 3 and 4.

Assignments

CH-Stretching Region. Assignment of the methine-stretching mode in **I**−**V** (Figures 1 and 2) is facilitated by the deuteriation of the methyl ester group, methoxy group (in **II**), and acetyl methyl group (in **V**), which removes most of the strong aliphatic CH-stretching absorption bands in the nondeuterated molecules[4,17,45] that overlap and obscure the methine-stretching absorption intensity. In **IV**−**VI**, the phenyl CH stretches lie above 3000 cm^{-1} and do not interfere with the aliphatic CH stretches. For each of the six molecules **I**−**VI**, for which an oxygen heteroatom is adjacent to the methine bond at R_1, a distinct absorption feature corresponding to an intense monosignate positive VCD band is observed in the region 2860−2960 cm^{-1}, assigned to the methine-stretching mode (Table 2). The frequency of the methine stretch is very sensitive to its environment, and the band tends to be broad in nature as compared to CH_2- and CH_3-group stretching modes.[4]

In the absorption spectra for the three molecules with a phenyl group located in the R_3 position (**IV**, **V**, and **VI**), the phenyl CH-stretching modes give rise to five characteristic bands (three dominant and two weak), which occur above 3000 cm^{-1}. In the corresponding VCD spectra, a consistent (+,−) couplet is observed at ∼3070 and ∼3040 cm^{-1} for **IV** and **V**, where there is only one phenyl group. In molecule **VI**, two phenyl groups are present, and a (+,−,+) pattern is observed in the VCD spectrum.

For **I** and **II**, a nondeuterated methyl group remains in the R_3 position. The absorption spectrum (Figure 1) for the methyl group exhibits a pattern of three bands. The highest-frequency band at ∼3000 cm^{-1} is assigned to the two nearly degenerate

TABLE 1: Frequencies, Intensities, and Assignments of CH- and OH-stretching Modes[a]

absorption[b]		VCD		
frequency (cm^{-1})	ϵ_{max} (10^3 cm^2 mol^{-1})	frequency (cm^{-1})	$\Delta\epsilon_{max} \times 10^3$ (10^3 cm^2 mol^{-1})	assignment[b]
		I. (*S*)-Methyl-d_3 Lactate		
3612	23	3615	−1.6	OH- -OCH_3
3555	108	3551	−7.5	OH- -O═C
2986	54	3002	0.5	C*CH_3 asym
		2985	−0.7	C*CH_3 asym
2940	25			C*CH_3 sym F. R.
		2932 (sh)	1.5	
2884	18	2880	3.1	C*H
		II. (*S*)-Methyl-d_3 2-(Methoxy-d_3)-propionate		
2992	56	3007	0.4	C*CH_3 asym
2942	26			C*CH_3 sym F. R.
2899 sh	21			
2878	31	2880	5.9	C*H
2809 sh		2809	0.6	
		III. Di(methyl-d_3) D-tartrate[b]		
3585 sh	30			OH- -OCH_3
		3545	−6.5	
3535	150			OH- -O═C
		3520	6.2	
2955	8			
2928	22	2930	5.6	C*H
		IV. (*S*)-Methyl-d_3 Mandelate		
3610 sh	10			OH- -OCH_3
3533	80	3542	−5.0	OH- -O═C
3109 sh	8			phenyl CH
3092	21			phenyl CH
3069	39	3069	0.6	phenyl CH
3036	41	3040	−0.6	phenyl CH
3011 ch	7			phenyl CH
2901	10	2901	1.8	C*H
		V. (*S*)-Methyl-d_3 *O*-(Acetyl-d_3)-mandelate		
3111 sh	7			phenyl CH
3094	17			phenyl CH
		3075	0.3	phenyl CH
3069	30			phenyl CH
3038	37	3047	−0.5	phenyl CH
3015	7			phenyl CH
2960	12	2960	2.3	C*H
		VI. (*S*)-Benzoin		
3619	3			OH free
3593	43	3595	0.9	OH- -O═C
3105	9			phenyl CH
3089	23	3070	−0.8	phenyl CH
3067	37			phenyl CH
3032	39	3030	0.8	phenyl CH
3009	8			phenyl CH
2895	11	2901	2.5	C*H
		VII. (*S*)-Methyl Chloropropionate		
3030 sh	16			(O)CH_3 asym
3001	45	3007	−1.6	(C)CH_3 asym + C*H + (O)CH_3 asym
2990 ch	41			(C)CH_3 asym + C*H
		2978	0.7	(C)CH_3 asym + C*H
2955	73			(O)CH_3 sym F. R.
2938	29	2940	1.1	(C)CH_3 sym F. R.
2905	10			
2872	10	2872	0.2	(C)CH_3 sym F. R.
2947	14			(O)CH_3 sym F. R.
		VIII. (*R*)-Methyl 3-Hydroxy-2-methylpropionate		
3634	39			OH- -OCH_3
3593	43	3593	0.9	OH- -O═C
		3580 sh	0.7	
3026 sh	18			(O)CH_3 asym
2992 sh	67	2986	1.9	(C)CH_3 asym; (C)CH_2 asym; (O)CH_3 asym
2974	82			(C)CH_3 asym, (C)CH_2 asym
		2959	−1.9	(C)CH_3 asym, (C)CH_2 asym
2953	137			(O)CH_3 sym F. R.
2944 sh	99	2939	1.0	(C)CH_3 sym F. R.; (C)CH_2 sym. F. R.; C*H
		2909	1.3	(C)CH_3 sym F. R.; (C)CH_2 sym. F. R.; C*H
2882	80			(C)CH_3 sym F. R.; (C)CH_2 sym. F. R.; C*H
2847 sh	23			(O)CH_3 sym F. R.

TABLE 1 (Continued)

absorption[b]		VCD		
frequency (cm^{-1})	ϵ_{max} (10^3 cm^2 mol^{-1})	frequency (cm^{-1})	$\Delta\epsilon_{max} \times 10^3$ (10^3 cm^2 mol^{-1})	assignment[b]
		IX. (*S*)-Methyl 3-Hydroxybutyrate		
3630 sh	10			OH- -OCH_3
		3593	0.8	
3565	38			OH- -O═C
		3445	−0.8	
3025 sh	18			(O)CH_3 asym
3003 sh	35			(C)CH_3 asym; (C)CH_2 asym; (O)CH_3 asym
2976	95	2983	−0.3	(C)CH_3 asym, (C)CH_2 asym
		2960	0.7	(C)CH_3 asym, (C)CH_2 asym
2955	87			(O)CH_3 sym F. R.
2936	49	2935	−0.5	(C)CH_3 sym F. R.; (C)CH_2 sym. F. R.; C*H
2903	41			(C)CH_3 sym F. R.; (C)CH_2 sym. F. R.; C*H
2886 sh	35	287	0.4	(C)CH_3 sym F. R.; (C)CH_2 sym. F. R.; C*H
2851 sh	17			(O)CH_3 sym F. R.
2810	5	2810	0.3	(C)CH_3 sym F. R.; (C)CH_2 sym. F. R.; C*H

[a] OH stretching frequencies measured for parent, nondeuterated species. [b] Abbreviations: sh, shoulder; asym, asymmetric; sym, symmetric; F. R., Fermi resonance component.

TABLE 2: Observed Frequencies and Intensities of Methine Stretches

	freq (cm^{-1})	ϵ_{max} (10^3 cm^2 mol^{-1})	$\Delta\epsilon_{max} \times 10^3$ (10^3 cm^2 mol^{-1})	$g \times 10^4$ (obs)
(*S*)-methyl-d_3 lactate (**I**)	2882	18	3.1	2.1
(*S*)-methyl-d_3 2-(methoxy-d_3)-propionate (**II**)	2878	22	5.6	2.1
di(methyl-d_3) D-tartrate (**III**)	2930	10	5.6	2.8
(*S*)-methyl-d_3 mandelate (**IV**)	2902	12	2.7	2.6
(*S*)-methyl-d_3 *O*-(acetyl-d_3)-mandelate (**V**)	2960	14	2.2	2.1
(*S*)-benzoin (**VI**)	2897	10	2.5	2.6

antisymmetric methyl stretches. A characteristic (+,−) VCD couplet is observed in the VCD spectrum of **I**, which arises from the antisymmetric methyl stretches coupling weakly with the methine stretch. The symmetric methyl stretch undergoes Fermi resonance[13,42] with the overtones of the antisymmetric methyl deformations, and contributes to the strong absorption band at ∼2940 cm^{-1}. The second Fermi component should occur near 2875 cm^{-1}, overlapping the broader methine-stretching absorption; however, since the distinct sharp 2940 cm^{-1} Fermi component has little or no corresponding VCD intensity, the intense positive VCD feature in **I** and **II** can be attributed solely to the methine stretch. The anisotropy ratios reported in Table 2 represent lower limits for **I** and **II**, since the contribution from the ∼2875 cm^{-1} symmetric stretching Fermi component to the absorption spectrum is uncertain.

For molecules **I** to **VI**, for which accurate measurements of both methine-stretching absorbance and VCD intensity can be made, the anisotropy ratio, $\Delta A/A$ (Table 2), lies between 2.1 and 2.8×10^{-4}, that is, within experimental error, the anisotropy ratios for these six molecules are essentially identical, and do not depend on the presence of a hydrogen-bonded ring.

Methyl 2-chloropropionate, **VII,** derives from the methyl lactate structure by substitution of chlorine for the R_1 hydroxyl group. Methyl 3-hydroxy-2-methylpropionate,**VIII,** and methyl 3-hydroxybutyrate, **IX,** can also be considered to be modifications of methyl lactate, **I**, in which a CH_2 group has been inserted between the chiral carbon atom and the R_1 hydroxyl group in **VIII**, and between the chiral carbon atom and the R_2 ester group in **IX**. The addition of the methylene group gives rise to significant changes in the absorbance and VCD spectra of **VIII** and **IX** compared to that of **I**. The methylene group contributes an additional antisymmetric stretch at ∼2976 cm^{-1} and symmetric stretching Fermi diad at ∼2944 and ∼2882 cm^{-1} in the CH-stretching absorbance spectra. The calculated normal modes for conformers of **VIII** and **IX** indicate extensive mixing among the methyl, methylene, and methine stretches. The methyl ester, which is not deuterated in **VII** − **IX**, also adds absorption features, two antisymmetric methyl ester stretches at ∼3025 and ∼3000 cm^{-1}, and a symmetric stretch assigned to the strong band at ∼2955 cm^{-1} and weaker Fermi resonance components including the feature at ∼2850 cm^{-1}.[46] The ester group CH stretches do not generate measurable VCD bands, as demonstrated by comparison of the VCD spectra of (*S*)-methyl lactate[8,45] and (*S*)-methyl-d_3 lactate.

For molecule **VII**, due to the chlorine atom at R_1, rather than an oxygen, the frequency of the methine stretch is expected to shift to ∼3000 cm^{-1},[47] as confirmed by our calculations, which show strong coupling of the methine stretch with the antisymmetric methyl (C*CH_3) stretches. A strong positive VCD feature is not measured in this region for **VII**. For molecules **VIII** and **IX**, our calculations demonstrate that the methine stretch couples with stretches of adjacent CH_2 and CH_3 groups and cannot be assigned to a specific band. The VCD spectra (Figure 3) for molecules **VII**−**IX** consist of a series of positive and negative features with no distinct overall intensity bias for **VII** and **IX** and some positive intensity bias for **VIII**; these VCD spectra are less intense overall compared to the dominant C*H-stretching VCD bands observed for molecules **I**−**VI** (Figures 1 and 2). It is obvious that a strong monosignate feature is not observed in the VCD spectra for molecules **VII**, **VIII** and **IX**.

OH-Stretching Region. The OH-stretching frequencies, intensities, and assignments are presented in Table 1 for nondeuterated **I**, **III**, **IV**, **VI**, **VIII**, and **IX**. Since the OH stretch does not significantly couple with the CH stretches, the data presented here for the nondeuterated molecules apply to the deuterated species, as confirmed by measurements on methyl-d_3 lactate.[30] In CCl_4 solution, the free aliphatic alcohol OH stretching band is located above 3620 cm^{-1}. When the OH is involved in a strong OH- -O═C hydrogen bond, the frequency of the stretch falls below 3600 cm^{-1}. When the OH is hydrogen-bonded to an OCH_3 oxygen, the frequency is decreased from that of a free OH stretch, but remains near 3600 cm^{-1}.

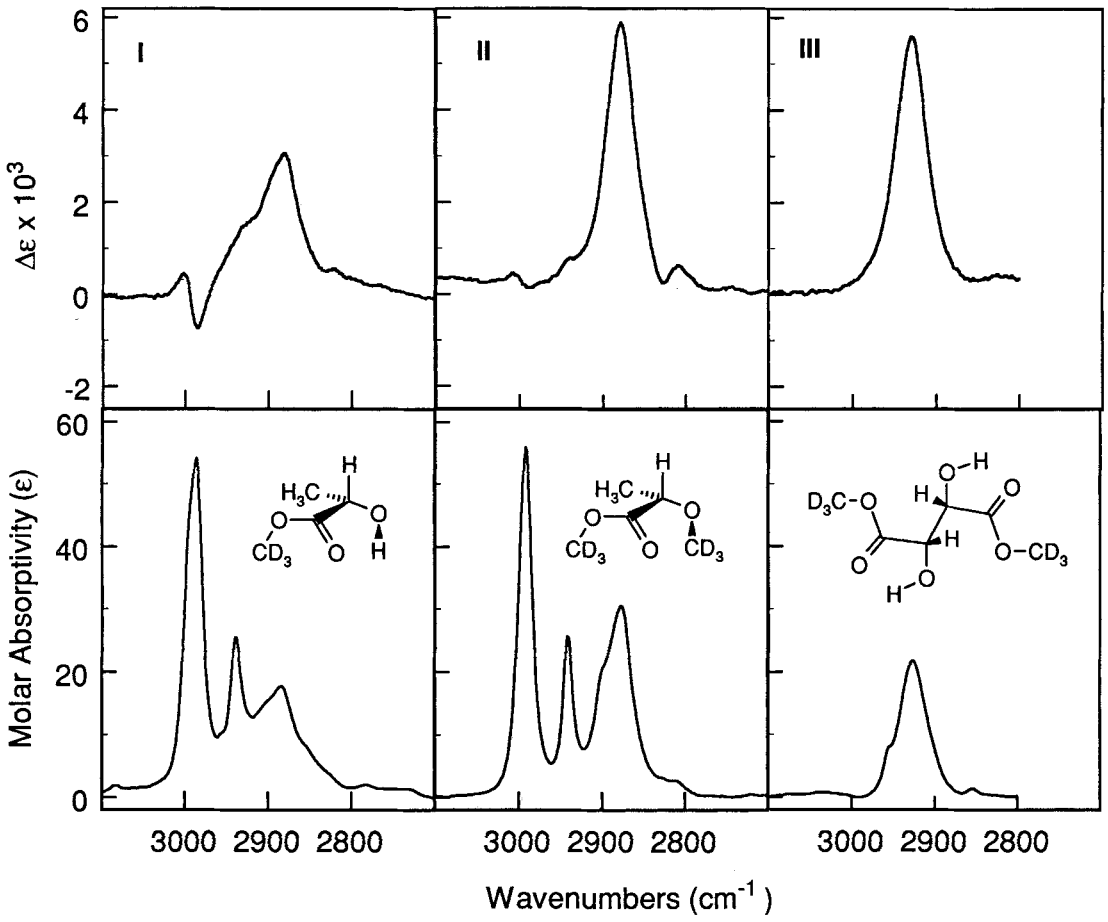

Figure 1. Comparison of CH-stretching molar absorptivity (ϵ) and VCD ($\Delta\epsilon$) spectra of (*S*)-methyl-d_3 lactate (**I**), (*S*)-methyl-d_3 2-(methoxy-d_3)-propionate (**II**), and di(methyl-d_3) D-tartrate (**III**), 0.01 M in CCl_4, 1.0 cm path length.

The OH-stretching spectra of **I**, **III**, **IV**, **VI**, **VIII**, and **IX**, measured for the parent, nondeuterated samples, exhibit two absorbance features, a strong band assigned to the OH- -O═C hydrogen-bonded stretching modes, and a weak band at higher frequency, assigned to the OH- -OCH_3 hydrogen-bonded OH stretch (**I**, **III**, **IV**, **VII**, and **IX**) or free OH stretch (**VI**) (Table 1). In (*S*)-methyl lactate (Figure 7), both bands give rise to negative VCD features, with similar features observed for (*S*)-methyl mandelate,[4] providing evidence for major OH- -O═C and minor OH- -OCH_3 conformers present in solution. In the absorbance spectrum of dimethyl D-tartrate (**III**),[29,43] a weak shoulder is observed at 3585 cm^{-1} and a stronger band at 3535 cm^{-1}. The corresponding VCD spectrum[29,43] exhibits a (−,+) couplet centered at 3532 cm^{-1}. The two hydrogen-bonded OH groups in **III** are chirally oriented about the C_2-axis, and couple to produce the (−,+) couplet.

For benzoin (**VI**) only the OH- -O═C hydrogen-bonded stretch exhibits negative VCD intensity, with no VCD observed for the free OH.[41] The spectrum for (*R*)-methyl 3-hydroxy-2-methylpropionate (Figure 12), **VIII**, exhibits two major absorbance features: a high-frequency band at 3634 cm^{-1} (free or OH- -OCH_3), and a lower frequency band at 3593 cm^{-1} (OH- -O═C), which exhibits weak negative VCD with a low-frequency negative shoulder. Finally, the absorbance spectrum of (*S*)-methyl 3-hydroxybutyrate,[30] **IX**, reproduced in Figure 14, exhibits a weak shoulder at 3630 cm^{-1} and a more intense feature at 3565 cm^{-1} that corresponds to a VCD couplet, indicative of more than one OH- -O═C hydrogen-bonded conformer and at least one OH- -OCH_3 hydrogen-bonded conformer present in solution.

The experimental OH-stretching absorption and VCD spectra for all the molecules with OH groups are thus consistent with multiple stable solution conformers for these molecules, with the OH- -O═C conformers most abundant.

Calculations and Interpretation

Ab initio molecular orbital calculations of optimized lowest-energy geometries, vibrational frequencies, and IR and VCD intensities were carried out on (*S*)-methyl-d_3 lactate, **I**, (*S*)-methyl-d_3 2-(methoxy-d_3)-propionate, **II**, (*S*)-methyl 2-chloropropionate, **VII,** (*R*)-methyl 3-hydroxy-2-methylpropionate, **VIII**, and (*S*)-methyl 3-hydroxybutyrate, **IX**, for the conformations shown in Figures 4 and 5. Geometry optimizations carried out with 6-31G(d) and 6-31$G^{(0.3)}$ basis sets yielded optimized structures with similar relative energies for the two basis sets; VCD intensity calculations with the vibronic coupling theory sum-over-states method (VCT) require the 6-31$G^{(0.3)}$ basis set.[26] For methyl lactate and methyl chloropropionate, density functional calculations (B3LYP) of geometries, force fields, and atomic polar tensors were also obtained, which were combined with atomic axial tensors from a VCT calculation for the same geometry and basis set to obtain rotational strengths. For the larger molecules, methyl-d_3 mandelate, **IV**, methyl-d_3 *O*-(acetyl-d_3)-mandelate, **V**, and benzoin, **VI**, low-energy conformations were surveyed by using a 3-21G basis set.[41] Geometry calculations with a 6-31G basis set on tartaric acid have been previously reported by Polavarapu.[48] For our study, geometries with intramolecular hydrogen-bonding to the carbonyl or the methoxy oxygen of the ester consistent with experiment, as well as various non-hydrogen-bonded orientations, were explored. The

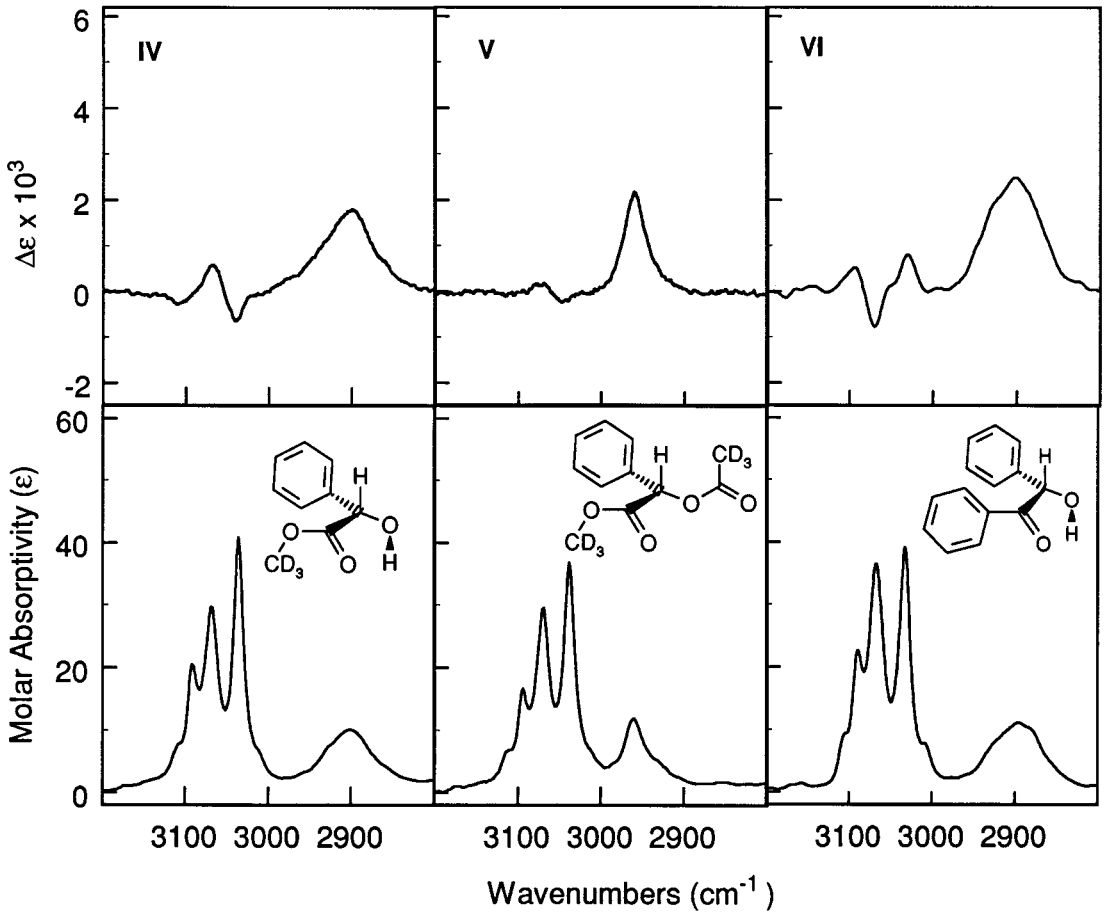

Figure 2. Comparison of CH-stretching molar absorptivity (ϵ) and VCD ($\Delta\epsilon$) spectra of (*S*)-methyl-d_3 mandelate (**IV**), (*S*)-methyl-d_3 *O*-(acetyl-d_3)-mandelate (**V**) and (*S*)-benzoin (**VI**), 0.01 M in CCl_4, 1.0 cm path length.

relative energies, structural parameters, and anisotropy ratios, calculated for the species fully deuterated except for the C*H and OH hydrogens, are compared in Tables 3 and 4. For ease of comparison between experiment and calculation, the frequencies in the calculated spectra have been uniformly scaled by 0.915 for the 6-31G$^{(0.3)}$ HF calculations and by 0.98 for the DFT calculations for the CH-stretching region, and by 0.906 for the OH stretches (6-31G$^{(0.3)}$ HF calculations).

Methyl-d_3 Lactate (I). Four conformers were calculated for (*S*)-methyl lactate (Figure 4), the lowest-energy conformer Ia with OH- -O═C hydrogen-bonding, conformers Ib and Ic with OH- -O(CH_3) hydrogen-bonding, which have similar energies, and a high-energy conformer with no hydrogen-bonding. In all four conformers, the closest O- -O(H) distance is ∼2.7 Å.

The dominant conformer in solution is conformer Ia, as clearly seen by the agreement between observed and calculated IR and VCD spectra for the nondeuterated molecule in both the mid-infrared region (Figure 6) and OH-stretching region (Figure 7). The mid-infrared calculations, which utilize DFT geometry, force field, and atomic polar tensors in conjunction with VCT calculations of the atomic axial tensors, demonstrate the quite favorable agreement between VCD intensities calculated with this method and experimental measurement in this region, which is comparable to recent demonstrations of magnetic field perturbation (MFP) DFT calculations of VCD intensity.[19] Our mid-IR VCD HF/6-31G$^{(0.3)}$ VCT calculations (not shown) deviate from experiment primarily for the mode at 1270 cm^{-1}, for which both the IR and VCD intensity are calculated to be too large. Unique features that can be attributed to conformers Ib or Ic cannot be identified from these mid-IR spectra. We note that the mid-IR spectra for (*S*)-methyl lactate were obtained for a sample 20 times more concentrated than that used for the hydrogen-stretching spectra, and thus the conformer populations may differ for the two samples.

The observed and calculated OH-stretching VCD for (*S*)-methyl lactate indicate the presence of a population of conformer Ib, giving rise to the OH- -O(CH_3) stretch at 3615 cm^{-1}. Conformer Ic is calculated to have a weak positive OH-stretching VCD; a contribution from this conformer would be obscured by the negative VCD from conformers Ia and Ib. Conformer Id lies at too high an energy to be sufficiently populated, and no evidence of free OH stretch is observed.

In the CH-stretching region (Figure 8), the Fermi resonance between the symmetric methyl stretch and overtone of the antisymmetric methyl deformations is responsible for the deviation between the observed and calculated absorbance patterns. For example, the intense absorbance for the unperturbed symmetric methyl stretch of Ia calculated at 2890 cm^{-1} (scaled frequency) corresponds to the two experimental Fermi resonance components at 2940 and ∼2880 cm^{-1}, the latter overlapped by the methine stretch. Comparison of observed and calculated VCD spectra in this region are again consistent with a dominant contribution from conformer Ia, which generates intense positive methine-stretching VCD and a (+,−) VCD couplet for the antisymmetric stretches weakly coupled to the methine stretch. Conformer Ib is calculated to have only weak positive methine-stretching VCD, at a frequency 30 cm^{-1} lower than for Ia; features unique to this conformer are not evident in the experimental spectra in this region. For conformer Ic, the methine stretch is calculated to lie 80 cm^{-1} above that of

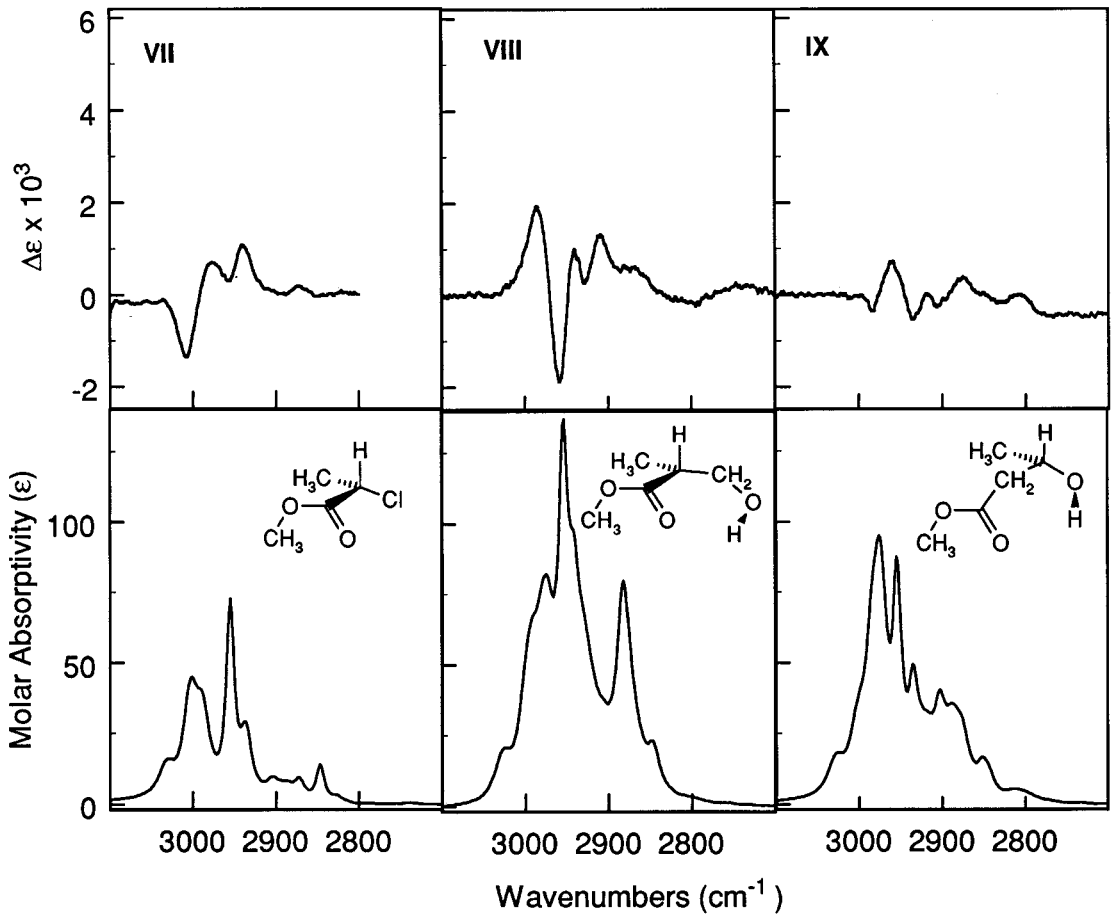

Figure 3. Comparison of CH-stretching molar absorptivity (ϵ) and VCD ($\Delta\epsilon$) spectra of (*S*)-methyl 2-chloropropionate (**VII**), (*R*)-methyl 3-hydroxy-2-methylpropionate (**VIII**), and (*S*)-methyl 3-hydroxybutyrate (**IX**), 0.01 M in CCl_4 for **VII**, 0.005 M for **VIII** and **IX**, 1.0 cm path length.

conformer Ia, with an intrinsic positive rotational strength half that of conformer Ia. For conformer Ia, the calculation at this level predicts a separation between the antisymmetric methyl stretches and the methine stretch smaller than experiment. If this is also the case for conformer Ic, the experimental frequency for the methine stretch of Ic may be lower than that calculated, with weaker coupling of the methine stretch with the antisymmetric methyl stretches. The methine stretch of Ic thus may be responsible for the positive shoulder in the experimental VCD spectrum at 2932 cm^{-1} (Figures 1 and 8). This shoulder lies $\sim$52 cm^{-1} higher in frequency than the methine stretch assigned to Ia, and its broad bandwidth precludes assignment to a methyl vibration. We note that for molecules **II** and **V**, for which a hydrogen-bonded conformer analogous to Ic is not possible, and for **III**, for which such a conformer is sterically improbable, no similar shoulder is observed on the intense positive methine-stretching band (Figures 1−2).

For these four conformers of methyl lactate, we find that conformers Ia and Ic are predicted to have large methine-stretching anisotropy ratios (Table 3), while that of conformer Ib is quite small. Conformer Id, which lacks a hydrogen-bond, is calculated to have a positive methine-stretching anisotropy ratio half that of conformer Ia. These results are similar to those previously obtained for conformers Ia and Id by Stephens and co-workers with MFP−VCD calculations.[17]

Methyl-d_3 2-(Methoxy-d_3)-propionate (II). The two lowest-energy conformations of (*S*)-methyl-d_3 2-(methoxy-d_3)-propionate (Table 3, Figure 4), IIa and IIb, differ by the rotation of the ester group. In both conformers the methoxy group is gauche to the C*H bond. Two other stable conformers (not shown), with the methoxy group trans to the methine and two orientations of the ester group corresponding to IIa and IIb, lie 8−12 kJ/mol in energy above IIa.[41] Comparison of the observed and calculated VCD spectra, Figure 9, shows that conformer IIa has a large positive methine-stretching VCD and is the dominant conformer in solution. The calculated methine intensities, anisotropy ratios, and O=C−C*-O dihedral angles (Table 3) calculated for IIa and IIb are similar to those for the corresponding structures Ia and Ib for (*S*)-methyl lactate. The VCD spectra of **II** provide both experimental and computational evidence that a hydrogen-bonded ring is not required for the generation of large methine-stretching VCD. We do find that the immediate environments of the methine bonds in the dominant conformers Ia and IIa are quite similar.

Di(methyl-d_3) D-Tartrate (III). Previous studies of the OH, C=O, and C−O stretches in dimethyl D-tartrate[29,43,49] relied on the VCD couplets in these regions, which arise from the in- and out-of-phase coupling of the pair of chirally oriented oscillators in each case, to ascertain the preferred solution conformation of this dimer-like molecule with C_2 symmetry. Although ab initio VCD intensity calculations for **III** have not been reported, ab initio geometry calculations on tartaric acid of Polavarapu and co-workers[48] indicated that in the most stable conformation the carboxyl groups are trans, with OH- -O=C hydrogen bonding between groups on the same chiral center. In contrast to the VCD couplets in the OH, C=O, and C−O stretching regions,[29,43,49] in the CH-stretching region, our data on di(methyl-d_3) D-tartrate reveal a single VCD band with anisotropy ratio similar to that for **I** and **II**. In this region, the intrinsic VCD intensity of each methine stretch obscures any

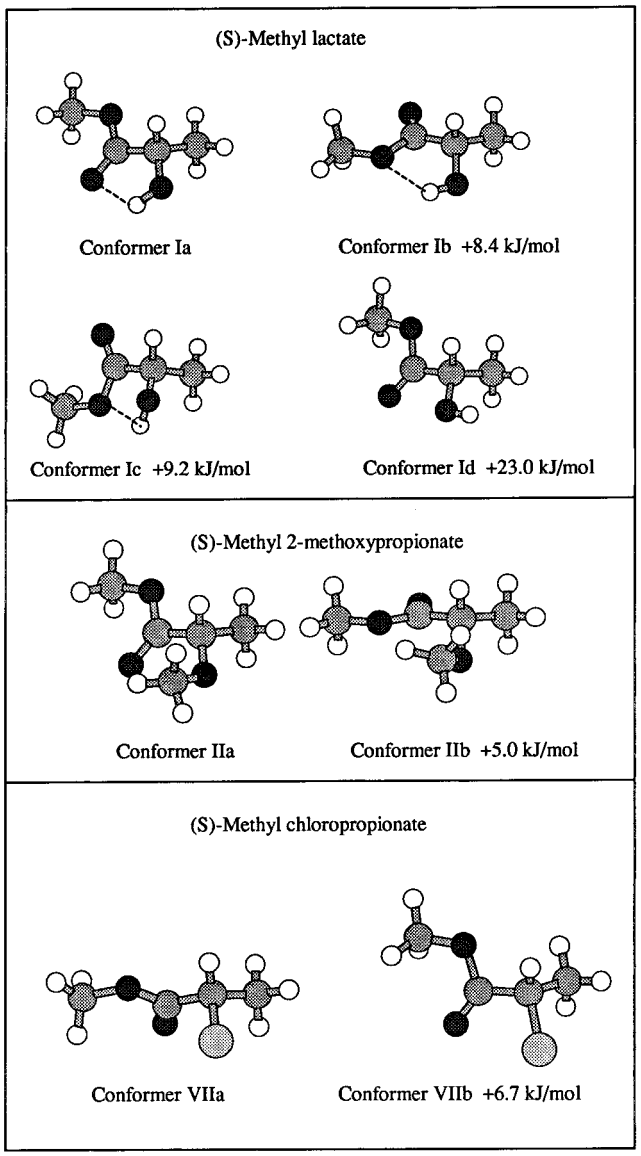

Figure 4. Calculated conformations and relative energies for (*S*)-methyl lactate, (*S*)-methyl 2-methoxypropionate, and (*S*)-methyl chloropropionate, with darkest shading for oxygen atoms, intermediate shading for carbon atoms, and white circles for hydrogens.

contribution from the coupling between the two methine stretches. The observed absorbance and VCD bands represent a superposition of the in- and out-of-phase vibrations of the two methine stretches, which are not resolved in either the IR or VCD spectrum. Coupling of the methine stretches generates VCD intensity contributions for these A and B symmetry modes with equal magnitude and opposite sign, and integration of the total methine-stretching intensity yields the sum of the intrinsic VCD for the two oscillators. Similarly, the integrated intensity of the observed absorption band is twice the intensity of an uncoupled methine stretch in **III**. Similar experimental results in this region are observed for tartaric acid in D_2O.[28] Our experimental CH-stretching VCD data for **III** are consistent with a conformer corresponding to that calculated for tartaric acid,[48] which also corresponds to conformation Ia for each chiral center.

(S)-Methyl-d_3 Mandelate (IV). Three unique conformations for (*S*)-methyl-d_3 mandelate, **IV**, were identified in our calculations, with orientations of hydroxy and ester groups and relative energies similar to those of Ia, Ib, and Id.[41] The single absorbance and large positive VCD feature in the aliphatic CH-stretching region are again consistent with a dominant

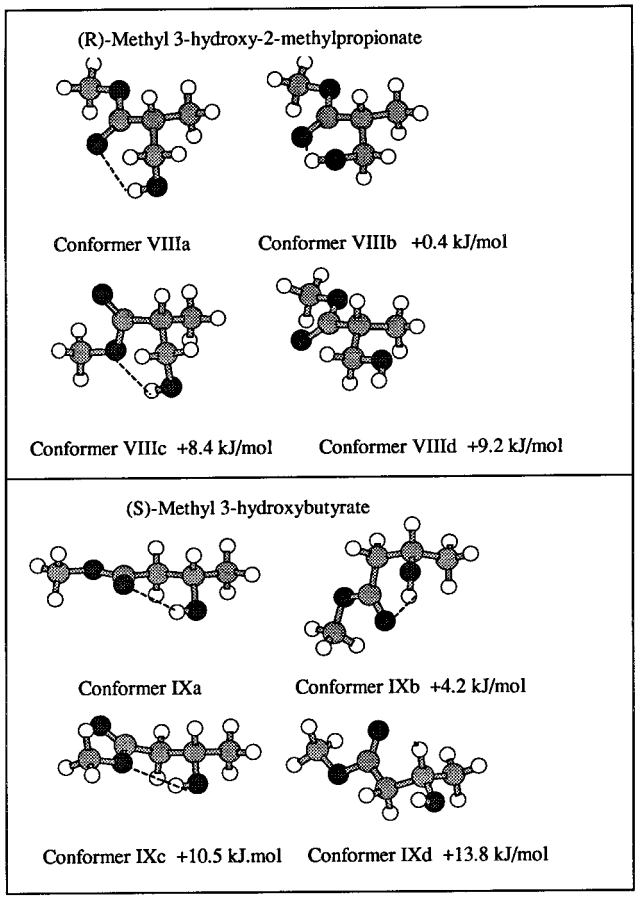

Figure 5. Calculated conformations of (R)-methyl 3-hydroxy-2-methylpropionate and (*S*)-methyl 3-hydroxybutyrate, with relative energies.

OH- -O=C conformer. The OH-stretching region indicates an additional minor contribution from the OH- -OCH_3 conformer analogous to Ib. A stable conformer similar to Ic was not found, and no high-frequency shoulder is observed on the methine-stretching VCD feature, in contrast to the VCD for **I**.

(*S*)-Methyl-d_3 *O*-(Acetyl-d_3)-mandelate (V). Calculations for methyl-d_3 *O*-(acetyl-d_3)-mandelate, **V**, found only two unique conformations differing in energy by 4.2 kJ/mol, in which the ester and HC*OR orientations correspond to conformers IIa and IIb of (*S*)-methyl methoxypropionate.[41] The VCD spectra and C*H-stretching anisotropy ratios are consistent with a dominant conformer analogous to IIa. This molecule provides a second example of large methine-stretching VCD in the absence of an intramolecularly hydrogen-bonded ring, but with a nearly planar O=CC*O arrangement.

(*S*)-Benzoin (VI). The two calculated lowest-energy conformers of benzoin, **VI**, differ in energy by ~20 kJ/mol, with geometries corresponding to conformers Ia and Id.[41] Both the OH- and CH-stretching VCD spectra are consistent with a single conformer analogous to Ia, although the absorbance spectra suggest a small amount of a conformer analogous to Id. In this case, this "free OH" orientation may be stabilized by interaction with the C*-phenyl group. For benzoin, we see that replacing the ester group with the phenyl ketone has little effect on the methine VCD intensity or anisotropy ratio (Table 2).

(*S*)-Methyl 2-Chloropropionate (VII). Two unique conformations, VIIa and VIIb, were found for **VII** at the Hartree−Fock level (Figure 4), whereas only conformer VIIa was obtained with a density functional (B3LYP) geometry optimization. The closest O−Cl distance is 3.2−3.6 Å in these structures.

TABLE 3: Calculated Frequencies and Anisotropy Ratios of Methine Stretches for Conformers with Deuterated Methyl and Methylene Groups

molecule	conformer	relative energy (kJ/mol)	freq (cm^{-1}) (scaled by 0.915)	$g \times 10^4$ (calculated)	∠O═C−C*−X (deg)[a]	∠O═C−C*−H (deg)
(*S*)-methyl lactate-d_6	Ia	0.0	2899	1.1	−3.3	−120.9
	Ib	+8.4	2861	0.1	−147.6	93.6
	Ic	+9.2	2977	1.2	146.2	30.5
	Id	+23.0	2897	0.6	−17.0	−135.4
(*S*)-methyl 2-methoxypropionate-d_9	IIa	0.0	2874	1.5	−8.3	−129.1
	IIb	+5.0	2872	0.1	−130.5	110.7
(*S*)-methyl 2-chloropropionate-d_6	VIIa	0.0	2993	−0.1	−100.4	148.5
	VIIb	6.7	2993	1.4	−25.2	−140.5
(*R*)-methyl 3-hydroxy-2-methylproprionate-d_8	VIIIa	0.0	2892	0.8	−15.5	−133.0
	VIIIb	+0.4	2902	0.7	−3.7	−121.1
	VIIIc	+8.4	2897	−0.6	−124.5	118.8
	VIIId	+9.2	2909	1.4	−12.3	−129.9
(*S*)-methyl 3-hydroxybutyrate-d_8	IXa	0.0	2918	−0.2		
	IXb	+4.2	2882	−0.3		
	IXc	+10.5	2864	−0.01		
	IXd	+13.8	2909	0.5		

[a] X = O for methyl lactate and methyl 2-methoxyproprionate; X = Cl for methyl 2-chloroproprionate; X = C(methylene) for methyl 3-hydroxy-2-methylproprionate.

TABLE 4: Calculated Frequencies and Anisotropy Ratios of OH Stretches for I, VIII, and IX

molecule	conformer	rel. energy (kJ/mol)	freq (cm^{-1}) (scaled by 0.906)	$g \times 10^5$ (calculated)	hydrogen bonding
(*S*)-methyl lactate-d_6	Ia	0.0	3551	−4.1	OH- -O═C
	Ib	+8.4	3602	−2.9	OH- -OCH_3
	Ic	+9.2	3596	+1.9	OH- -OCH_3
	Id	+23.0	3607	−1.8	free OH
(*R*)-methyl 3-hydroxy-2-methylpropionate-d_8	VIIIa	0.0	3579	+2.2	OH- -O═C
	VIIIb	+0.4	3587	−4.1	OH- -O═C
	VIIIc	+8.4	3604	+1.7	OH- -OCH_3
	VIIId	+9.2	3619	−1.9	free OH
(*S*)-methyl 3-hydroxybutyrate-d_8	IXa	0.0	3577	+3.8	OH- -O═C
	IXb	+4.2	3569	−8.3	OH- -O═C
	IXc	+10.5	3601	+0.6	OH- -OCH_3
	IXd	+13.8	3604	+9.5	free OH

The presence of the chlorine substituent moves the methine stretch up in frequency to the region of the antisymmetric methyl stretches. The positive VCD features at 2940 and 2872 cm^{-1} are ascribed to Fermi resonance components of the symmetric methyl stretch. The high-frequency (−,+) intensity arises from the coupling of the methine and antisymmetric methyl stretches. In VIIa, with almost perpendicular C═O and C*−Cl bonds, the methine-stretching anisotropy ratio (for the -d_6 isotopomer) is calculated to be small and negative (Table 3), whereas VIIb, with a more eclipsed arrangement of these bonds, is again calculated to have a large positive methine-stretching anisotropy ratio. For **VII**, we calculated spectra for the methyl-d_3 ester to eliminate any effects in the calculation of coupling between the methyl groups, since the experimental data show no VCD intensity arising from the ester methyl group modes. The calculated VCD intensity for conformer VIIa, Figure 10, reproduces the sign pattern for the high-frequency (−,+) feature and the positive symmetric methyl stretch, but includes a negative component not apparent in the observed spectrum, arising from the third component of the coupled antisymmetric methyl and methine stretches. Additional positive methine-stretching VCD intensity at ∼2980 cm^{-1} from a ∼30% contribution from conformer VIIb improves the fit between experiment and calculation (Figure 10), as does including the effects of the Fermi resonance to move most of the calculated positive symmetric methyl VCD intensity to 2940 cm^{-1}. Calculations of **VII** utilizing the DFT geometry, force field, and atomic polar tensors yield somewhat better agreement with experiment for conformer VIIa, when the effects of the Fermi resonance are included to redistribute the positive VCD intensity calculated for the mode (∼2890 cm^{-1}) with a predominant contribution from (C*CH_3) methyl symmetric stretch (Figure 11).

(*R*)-Methyl 3-Hydroxy-2-methylpropionate (VIII). Four conformers were considered for molecule **VIII** (Figure 5). The two lowest-energy conformers, with OH- -O═C hydrogen-bonding, lie very close in energy. The VCD spectra are consistent with an approximately equal mixture of VIIIa and VIIIb as the dominant conformers. In the OH-stretching region, these two conformers have VCD intensities of opposite sign, with VIIIb at a slightly lower frequency (Figure 12). A 54:46 ratio (the calculated Boltzmann populations) of VIIIa:VIIIb yields small net negative OH-stretching VCD intensity, in agreement with experiment. We note that our calculations consistently yield both absorbance and VCD intensities in this region that are smaller than experiment. The high-frequency shoulder in the absorbance spectrum of **VIII** arises from a small contribution from conformers such as VIIIc and the analogous conformer to VIIIb with OH- -OCH_3 hydrogen-bonding, which are calculated to have a large absorbance intensity, but weak VCD that would largely cancel for two such conformers (see, for example, the calculated spectrum of XIc in Figure 15). The experimental data do not show absorbance features that can be attributed to free OH conformers such as VIIId. In the CH-stretching region, the VCD pattern is also consistent with dominant contributions from VIIIa and VIIIb (Figure 13); one must again take into account the methyl and methylene symmetric stretching Fermi resonance to redistribute some of the calculated absorbance and positive VCD intensity near 2900 cm^{-1} to ∼2930 and 2970 cm^{-1}. It is of interest to note that the

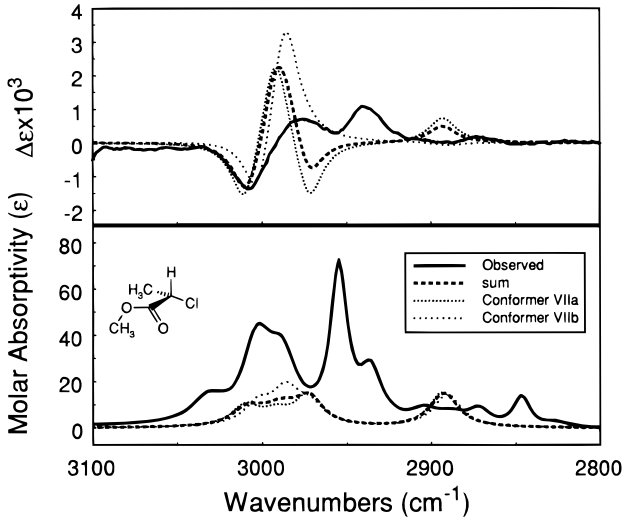

Figure 10. Comparison of experimental molar absorptivity (ϵ) and VCD ($\Delta\epsilon$) spectra of (*S*)-methyl chloropropionate (**VII**) in the CH-stretching region with calculated spectra for conformers VIIa and VIIb and composite sum spectra 70% VIIa and 30% VIIb (HF/6-31G$^{(0.3)}$ VCT calculation).

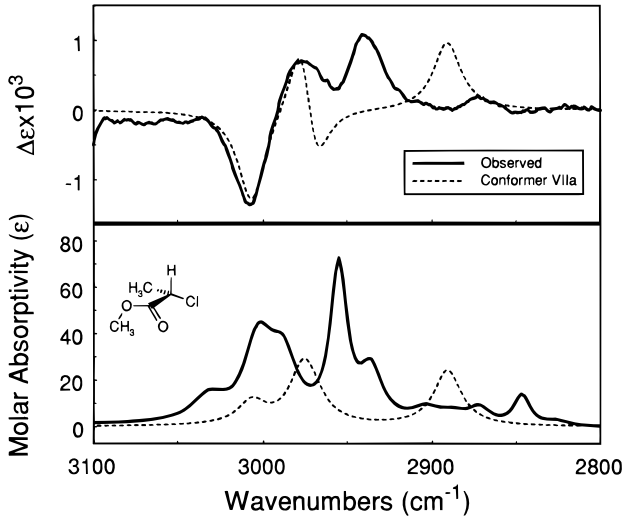

Figure 11. Comparison of experimental molar absorptivity (ϵ) and VCD ($\Delta\epsilon$) spectra of (*S*)-methyl chloropropionate (**VII**) in the CH-stretching region with calculated spectra for conformer VIIa with B3LYP/DFT geometry, force field and atomic polar tensors, and VCT atomic axial tensors.

calculated anisotropy ratios (Table 3) for the uncoupled methine stretches in these four conformers of **VIII** are fairly large and positive, with the largest values for the more planar, cis arrangements of O=CC*C(H_2). Although the methine stretch couples extensively with the methyl and methylene modes in **VIII**, there is an overall net positive VCD intensity bias in the observed spectrum, and in the calculated VCD spectrum of each conformer, which can be attributed to the intrinsic VCD contribution from the methine stretching motion.

(*S*)-Methyl 3-Hydroxybutyrate (IX). Molecule **IX** exhibits the weakest overall CH-stretching VCD intensity. For the four conformers considered here, the calculated anisotropy ratio for the uncoupled methine stretch is small and negative for IXa, IXb, and IXc, and positive for conformer IXd, where the carbonyl oxygen is again near the C*H bond. The OH-stretching (+,−) VCD couplet[30] (Figure 14) is reproduced by the calculated spectrum for a 2:1 mixture of the lowest-energy conformers IXa and IXb, which exhibit VCD of opposite signs.

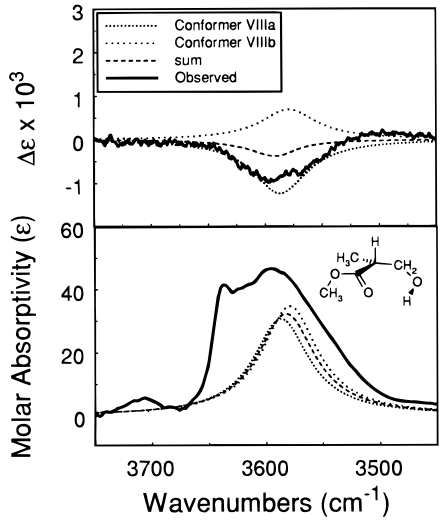

Figure 12. Comparison of experimental molar absorptivity (ϵ) and VCD ($\Delta\epsilon$) spectra of (*R*)-methyl 3-hydroxy-2-methylpropionate (**VIII**) in the OH-stretching region with calculated spectra for conformers VIIIa and VIIIb and composite summed spectra 54% VIIIa/46% VIIIb (HF/6-31G$^{(0.3)}$ VCT calculation).

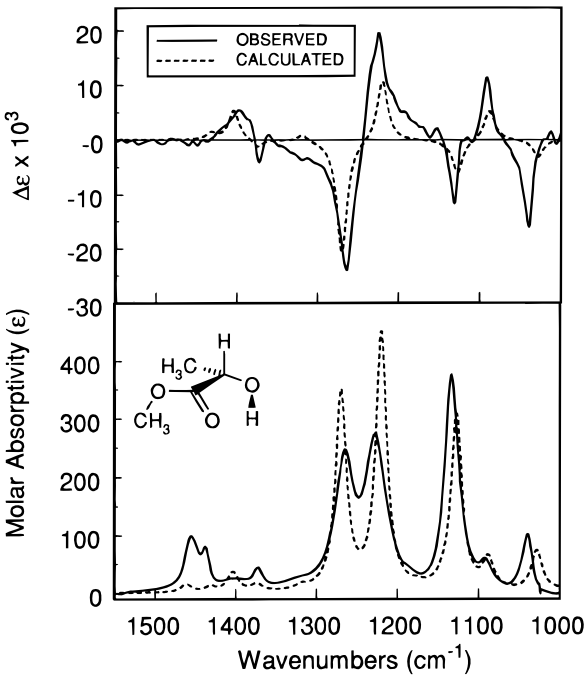

Figure 6. Comparison of observed and calculated molar absorptivity (ϵ) and VCD ($\Delta\epsilon$) spectra of (*S*)-methyl lactate in the mid-IR region. Calculated spectrum is for conformer Ia, with B3LYP/DFT geometry, force field and atomic polar tensors, and VCT atomic axial tensors. Experimental conditions: 0.2 M in CCl_4, 100 μm path length, 4.0 cm^{-1} resolution, 4 h collection for each enantiomer.

In Figure 15 we show the composite spectrum for a 6:3:1 mixture of IXa:IXb:IXc to illustrate the contribution from an OH- -OCH_3 conformer to the absorbance and VCD spectra. The observed CH-stretching VCD pattern (Figure 3) is not well reproduced by this composite of conformer spectra (Figure 16). Reproducing such a weak spectrum, where there is apparently considerable cancellation among VCD bands from numerous contributing conformers, requires a more accurate calculation of the normal modes in this region and a consideration of a more extensive set of conformers, which is beyond the scope of the present study of factors contributing to methine-stretching VCD intensity. For the conformers explored here, we find that

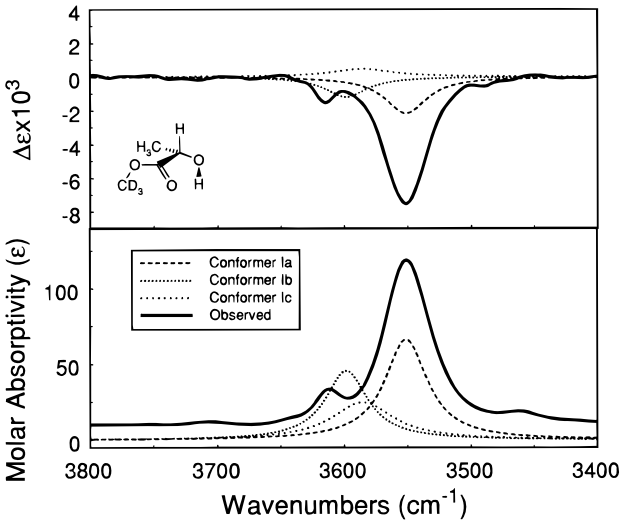

Figure 7. Comparison of experimental molar absorptivity (ϵ) and VCD ($\Delta\epsilon$) spectra of (*S*)-methyl lactate in the OH-stretching region with calculated spectra for conformers Ia, Ib, and Ic (HF/6-31G$^{(0.3)}$ VCT calculation). Experimental conditions: 0.005 M in CCl_4, 1 cm path length.

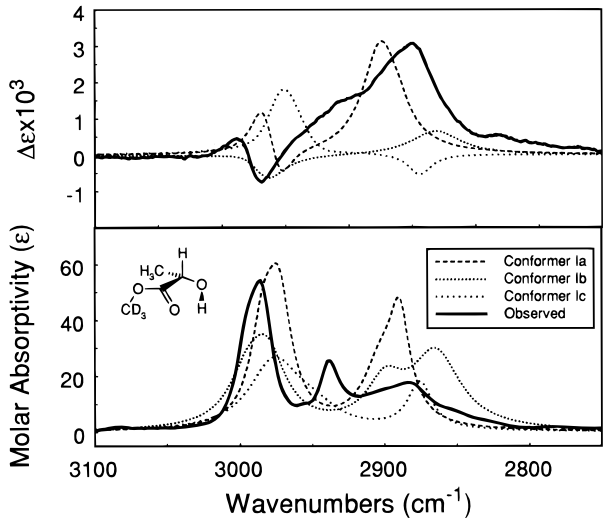

Figure 8. Comparison of experimental molar absorptivity (ϵ) and VCD ($\Delta\epsilon$) spectra of (*S*)-methyl-d_3 lactate (**I**) in the CH-stretching region with calculated spectra for conformers Ia, Ib, and Ic (HF/6-31G$^{(0.3)}$ VCT calculation).

the overall calculated VCD intensity is conservative for the conformers (IXa, IXb, and IXc) with small intrinsic methine VCD contributions.

Discussion

The VCD spectra of this set of molecules, coupled with ab initio geometry and intensity calculations, provide clear information on their solution conformations. For molecules with OH groups, the VCD spectra in the OH- and CH-stretching regions provide complementary data on minor conformer populations, as well as identification of the most abundant species. The ab initio calculations carried out for the gas-phase structures provide unambiguous assignments of VCD features, and reasonable estimates of relative conformer populations can be made by comparing composite calculated spectra with experiment. We note that the calculated relative energies do not yield correct solution conformer population distributions based solely on Boltzmann populations, since the relative stabilization of OH- -O═C, OH- -OCH_3, and free OH conformations are not well reproduced in the calculations. However, the calculated relative abundance and energy sequence of conformers with similar types of hydrogen-bonding is consistent with experiment, as shown for **VIII** and **IX**.

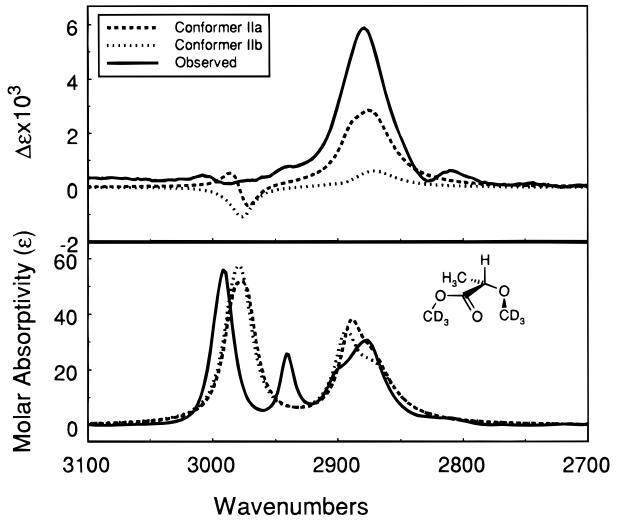

Figure 9. Comparison of experimental molar absorptivity (ϵ) and VCD spectra of (*S*)-methyl-d_3 2-(methoxy-d_3)-propionate (**II**) in the CH-stretching region with calculated spectra for conformers IIa and IIb (HF/6-31G$^{(0.3)}$ VCT calculation).

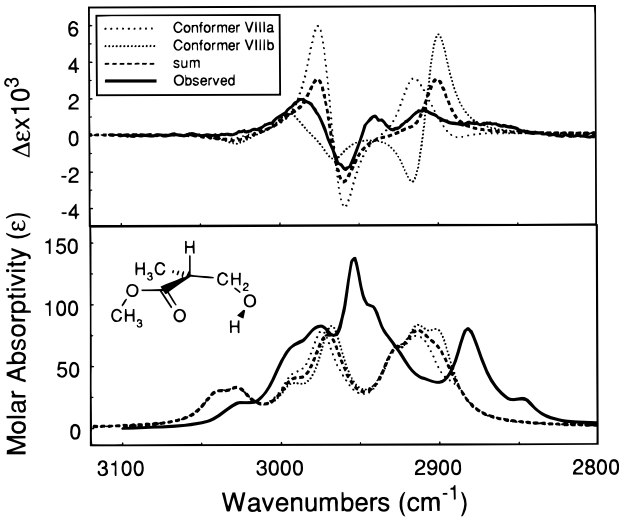

Figure 13. Comparison of experimental molar absorptivity (ϵ) and VCD ($\Delta\epsilon$) spectra of (*R*)-methyl 3-hydroxy-2-methylpropionate (**VIII**) in the CH-stretching region with calculated spectra for conformers VIIIa and VIIIb and composite summed spectra 54% VIIIa/46% VIIIb (HF/6-31G$^{(0.3)}$ VCT calculation).

The OH-stretching VCD spectra for molecules **I**, **III**, **IV**, **VI**, **VII**, **VIII**, and **IX** consist of both positive and negative features. The OH- -O═C stretch is the most dominant feature in this region. The intense, broad, negative OH-stretching VCD for **I**, **IV**, and **VI** is characteristic of conformers analogous to Ia, and serves as a VCD marker band for this conformation and configuration. In **III**, the vibrational coupling of the chirally oriented OH bonds results in a fairly conservative VCD couplet[29] that obscures smaller intrinsic VCD from each local oscillator. For both **VIII** and **IX**, the OH-stretching VCD spectra are consistent with a composite of two oppositely signed contributions. In Figure 17 we compare the environment of the OH bond in OH- -O═C conformers calculated to have either negative or positive OH-stretching VCD in **I**, **VIII**, and **IX**, by viewing

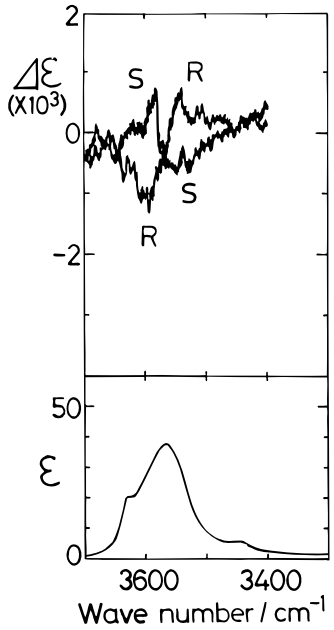

Figure 14. Experimental OH-stretching molar absorptivity (ϵ) and VCD ($\Delta\epsilon$) spectra of (*R*)- and (*S*)-methyl 3-hydroxybutyrate (**IX**), 0.008 M in CCl_4 (reproduced with permission from the Chemical Society of Japan, from ref 30, copyright 1984).

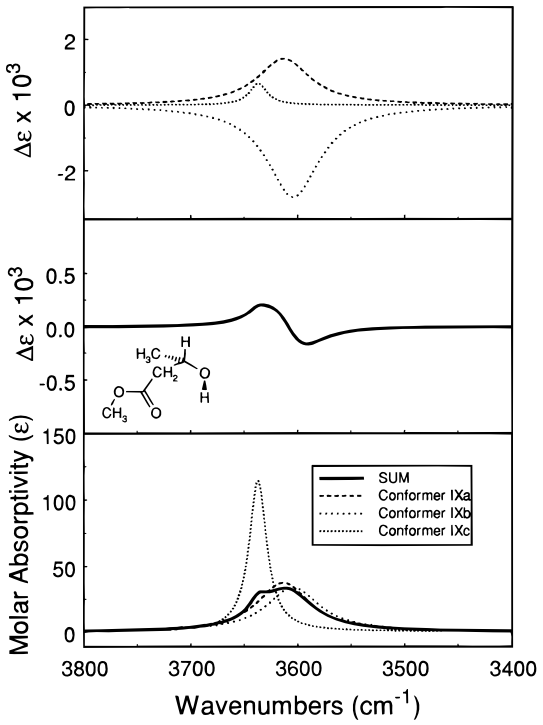

Figure 15. Calculated OH-stretching molar absorptivity (ϵ) and VCD ($\Delta\epsilon$) spectra of (*S*)-methyl 3-hydroxybutyrate (**IX**) conformers IXa, IXb, and IXc and composite summed spectra 70% IXa: 30% IXb: 10% IXc (HF/6-31G$^{(0.3)}$ VCT calculation).

stereoprojections of the calculated structures down the OH bond. The approximately mirror-image environments of the OH oscillator in the (VIIIa, VIIIb) conformer pair and the (IXa, IXb) conformer pair are clearly seen from this view, and provide an understanding of the origin of the oppositely signed OH-stretching VCD for each pair. We also note some similarity in the OH environment for VIIIa and Ia (Figure 17) which exhibit the same OH-stretching VCD sign, whereas a similar correlation between conformers of **I** and **IX** is not evident.

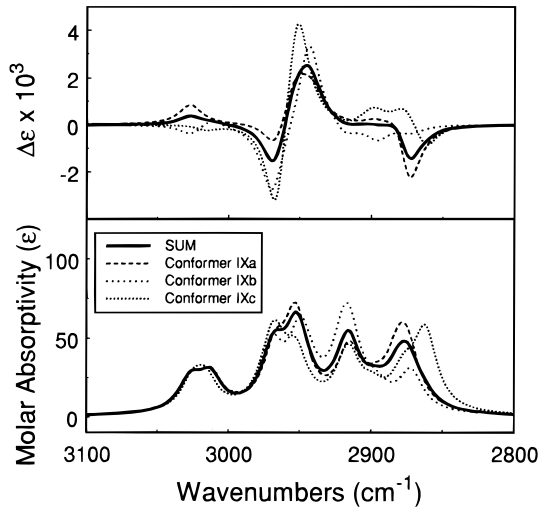

Figure 16. Calculated CH-stretching molar absorptivity (ϵ) and VCD ($\Delta\epsilon$) spectra of (*S*)-methyl 3-hydroxybutyrate (**IX**) conformers IXa, IXb, and IXc and composite summed spectra 60% IXa: 30% IXb: 10% IXc (HF/6-31G$^{(0.3)}$ VCT calculation).

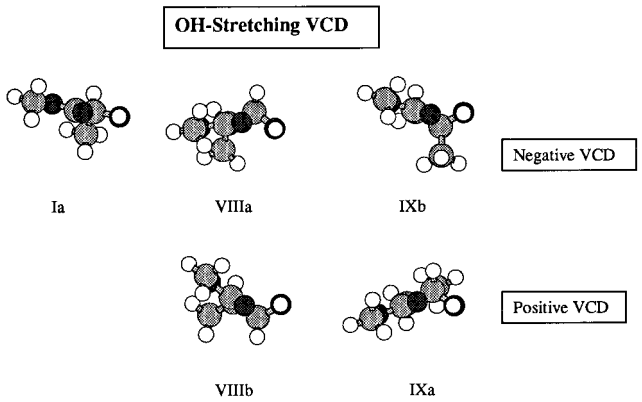

Figure 17. Comparison of OH-bond environments for positive and negative VCD. Each stereoprojection is viewed down the OH-bond at the right side of the structure, with darkest shading for oxygen atoms, intermediate shading for carbon atoms, and white circles for hydrogens.

The methine-stretching VCD anisotropy ratios (g) measured for **I**−**VI** are all $\sim 2.4 \times 10^{-4}$, independent of any intramolecular hydrogen-bonded rings. For all six of these molecules, the lowest energy conformation is similar to those shown for Ia or IIa, for which positive methine-stretching VCD with $g \sim 1.2 \times 10^{-4}$ is calculated. In these lowest energy conformers, the O═C−C*-O bonds form a cis, nearly coplanar arrangement (calculated dihedral angles: Ia, −3.3°; IIa, −8.3°; IVa, −13°; Va, −11°; VIa, 28°; O- -O distances are all ∼2.7 Å). We note that for conformer VIIb, for which a large positive methine-stretching VCD is again calculated, the O═C−C*−Cl dihedral angle is −25°, and for all three conformers (VIIIa, VIIIb, and VIIId) of **VIII** with large calculated positive methine-stretching anisotropy ratios the O═C−C*−C(methylene) dihedral angles are −15.5° or smaller. For conformer Id, with no hydrogen bond, the O═C−C*−O dihedral angle is −8.3°, and the calculated anisotropy ratio is half that of Ia. In contrast, the conformers with a trans, approximately coplanar O═C−C*−X arrangement (Ib, IIb, VIIa) all are calculated to have a very small methine-stretching VCD anisotropy ratio, as demonstrated experimentally by the nearly conservative CH-stretching VCD spectrum of **VII**. Thus, although the presence of a ring adjacent to the methine bond closed by hydrogen bonding is not required for intense methine-stretching VCD, the approximately cis planar arrangement of O═C−C*−X bonds that occurs for such closed rings, and for

IIa and Va, defines the local chiral environment that leads to large methine-stretching VCD. From the calculations on **VII** and **VIII**, we find that a carbon or chlorine atom can replace the oxygen at R_1 and still yield moderately large positive methine-stretching VCD, but that this intensity will be spread out among all the normal modes to which the C*H stretching motion contributes, as observed in the positively biased spectrum of **VIII**, which lacks a characteristic methine-stretching VCD feature. As seen from the calculated anisotropy ratios of **IX**, insertion of a methylene group between the chiral carbon and the carboxylate dramatically alters the methine-stretching VCD.

We note that although utilizing DFT geometry, force field and atomic polar tensors in the VCT intensity calculations improved the agreement between observed and calculated spectra in the mid-IR region below 1500 cm^{-1}, for the hydrogen-stretching regions similar DFT calculations gave poorer agreement with experiment than our HF/6-31G$^{(0.3)}$ VCT calculations for most of the molecules studied. For example, although the (+,−) VCD pattern was obtained in the DFT calculations for the antisymmetric stretches of (*S*)-methyl-d_3 lactate, the negative component was much larger than the positive one.

Conclusions

This study has demonstrated the utility of VCD in the hydrogen-stretching regions, combined with ab initio calculations of geometries and spectra, in identifying solution conformation and configuration. For the molecules with OH groups, the OH-stretching region, due to the small number of chromophores, provides the most direct information on solution conformers. However, we find that the CH- and OH-stretching regions can provide complementary information.

Methine-stretching VCD is most intense for an approximately cis planar arrangement of O═C−C*−X bonds, where X = O or N (as shown from previous studies on amino acids, amino acid-transition metal complexes, and peptides[8,9,11]), and the observation of intense, broad VCD in the CH-stretching region serves as a marker for configuration and conformation for a methine in a cis planar O═C−C*−X environment. When X is part of an OH group, the intense hydrogen-bonded OH-stretching VCD is also a marker for this cis planar geometry with OH- -O═C hydrogen bonding. For X = Cl, large positive methine-stretching VCD was calculated for such a cis planar conformation, but this conformation is not abundant in solution. For X = C, the methine-stretching VCD itself is fairly large and positive, but more extensive coupling of the methine stretch with CH stretches at R_1 and R_3 (Scheme 2) results in a distribution of the intrinsic methine-stretching VCD intensity across the aliphatic CH-stretching modes, producing a VCD intensity bias, but no single methine marker band. An sp^2 carbon at R_2 as part of a carbonyl, or, as previously demonstrated, a phenyl group,[4] is essential for large methine-stretching VCD. When sp^3 carbons occupy both the R_2 and R_3 positions, the methine-stretching VCD intensity is greatly reduced, even with a heteroatom at R_1.

The ambiguity in identifying methine-stretching features arising from minor conformations and in accurately measuring the anisotropy ratios, due to methine coupling with the C*CH_3 group in **I**, **II**, and **VII**, or the C*CH_3 and C*CH_2 groups in **VII** and **IX**, could be eliminated by additional deuteration. Such syntheses will be pursued in the future.

Finally, the agreement between observed and calculated VCD features for the most abundant conformers for this set of molecules provides a sound basis for employing the VCT sum-over-states formalism and computational methodology in calculations of vibrational transition current density for vibrations in the hydrogen-stretching regions. The methine-stretching TCD for the four conformations of methyl lactate has been calculated and will be reported separately.[50]

Appendix: Synthetic Procedures

General Procedure for Transesterification: (*R*)-Methyl-d_3 lactate. To 1.017 g of (*R*)-methyl lactate in 3 mL of methanol-d_4 was added 0.075 g of 10-camphorsulfonic acid, and the resulting mixture was heated at 65 °C for 24 h. Solvent was distilled from the reaction, an additional 3 mL of methanol-d_4 was added, and the reaction mixture was heated for an additional 24 h at 65 °C. The resulting mixture was partitioned between brine and ether, concentrated and purified by bulb-to-bulb distillation (86 °C, 40 mmHg) to give 0.317 g (30% yield) of (**I**): ^{1}H NMR ($CDCl_3$) d 1.41 (d, J = 7.2 Hz, 3H), 2.72 (d, J = 5.5 Hz, 1H), 4.28 (dq, J = 5.4, 6.8 Hz, 1H); $[a]_D$ −2.65 (c = 0.91, $CHCl_3$).

A) (*S*)-Methyl-d_3 lactate (I): $[a]_D$+3.09 (c = 0.81, $CHCl_3$).

B) (*R*)-Methyl-d_3 2-(methoxy-d_3)-propionate. (*R*)-methyl 2-(methoxy-d_3)-propionate (0.691 g) gave 0.360 g (51% yield) of (**II**): bp 95 °C (70 mmHg), ^{1}H NMR ($CDCl_3$) d 1.40 (d, J = 6.8 Hz, 3H), 3.89 (q, J = 6.7 Hz, 1H); ^{13}C NMR ($CDCl_3$) 18.39, 76.24, 173.61; $[a]_D$ +73.02 (c = 1.16, $CHCl_3$).

C) (*S*)-Methyl-d_3 2-(methoxy-d_3)-propionate (II): $[a]_D$ −67.23 (c = 2.38, $CHCl_3$).

D) Di(methyl-d_3) D-tartrate (III). Dimethyl D-tartrate (1.220 g), gave 1.128 g (90% yield) of (**III**): bp 145 °C (1.5 mmHg), ^{1}H NMR ($CDCl_3$) d 3.17 (d, J = 7.1 Hz, 2H), 4.56 (d, J = 7.1 Hz, 2H); ^{13}C NMR ($CDCl_3$) d 72.0, 171.8; $[a]_D$ −19.8 (c = 1.27, H_2O).

E) Di(methyl-d_3) L-tartrate: $[a]_D$ +19.9 (c = 0.94, H_2O).

F) (*S*)-Methyl-d_3 mandelate (IV). (*S*)-methyl mandelate (0.896 g) gave 0.828 g (91% yield) of (**IV**): bp 124 °C (1.5 mmHg), ^{1}H NMR ($CDCl_3$) d 3.53 (d, J = 5.5 Hz, 1H), 5.18 (d, J = 5.1 Hz, 1H), 7.3−7.5 (m, 5H) ppm; ^{13}C NMR ($CDCl_3$) d 72.7, 126.6, 128.46, 128.57, 138.2, 174.1 ppm; $[a]_D$ +140 (c = 0.81, MeOH).

G) (*R*)-Methyl-d_3 mandelate: $[a]_D$ −129 (c =0.74, MeOH).

H) (*R*)-Methyl-2-(methoxy-d_3)-propionate. To 0.903 g (8.7 mmol) (*R*)-methyl lactate in 7 mL of diethyl ether was added 2.31 g (10 mmol) of silver oxide, and 1.4 mL of methyl-d_3 iodide. The mixture was heated to reflux for 4 days after which filtration, concentration, and bulb-to-bulb distillation (95 °C, 70 mmHg) gave 0.692 g (67% yield) of the title compound: ^{1}H NMR ($CDCl_3$) d 1.39 (d, J = 6.7 Hz, 3H), 3.75(s, 3H), 3.88 (q, J = 6.9 Hz, 1H); ^{13}C NMR ($CDCl_3$) 18.37, 51.90, 76.22, 173.57. The S enantiomer was prepared in a similar manner.

I) (*S*)-Methyl-d_3 *O*-(acetyl-d_3)-mandelate (V). To 0.282 g (*S*)-methyl-d_3 mandelate in pyridine (3 mL) at 0 °C was added 0.24 mL of acetyl-d_3 chloride. After stirring 30 min the mixture was treated with water and ether (15 mL), washed with 10% HCl (3 × 15 mL), saturated bicarbonate, and brine. The organics were dried over magnesium sulfate, filtered, concentrated, and purified by flash chromatography (3:1 hexanes: ethyl acetate) to give 0.330 g (93% yield) of (**V**): ^{1}H NMR ($CDCl_3$) d 5.93 (s, 1H). 7.3−7.5 (m, 5H) ppm; ^{13}C NMR ($CDCl_3$) d 74.1, 127.3, 128.5, 128.9, 133.5, 168.9, 169.8 ppm; $[a]_D$ +136 (c = 1.05, $CHCl_3$).

J) (*R*)-Methyl-d_3 *O*-(acetyl-d_3)-mandelate: $[a]_D$ −126 (c = 0.92, $CHCl_3$).

Acknowledgment. The authors acknowledge support of this work from the National Institutes of Health (GM-23567) and

the New York State Center for Advanced Technology in Computer Applications and Software Engineering at Syracuse University.

References and Notes

(1) Nafie, L. A. *Annu. Rev. Phys. Chem.* **1997**, *48*, 357−386.
(2) Nafie, L. A. *Appl. Spectrosc.* **1996**, *50* (5), A14−A26.
(3) Freedman, T. B.; Nafie, L. A. In *Modern Nonlinear Optics, Part 3*; Evans, M., Kielich, S., Eds.; John Wiley & Sons: New York, 1994; Vol. 85, pp 207−263.
(4) Freedman, T. B.; Balukjian, G. A.; Nafie, L. A. *J. Am. Chem. Soc.* **1985**, *107*, 6213−6222.
(5) Freedman, T. B.; Ragunathan, N.; Alexander, S. *Faraday Discuss.* **1994**, 131−149.
(6) Long, F. Ph.D. Dissertation, Syracuse University, Syracuse, NY, 1998.
(7) Paterlini, M. G.; Freedman, T. B.; Nafie, L. A.; Tor, Y.; Shanzer, A. *Biopolymers* **1992**, *32*, 765−782.
(8) Oboodi, M. R.; Lal, B. B.; Young, D. A.; Freedman, T. B.; Nafie, L. A. *J. Am. Chem. Soc.* **1985**, *107*, 1547−1556.
(9) Zuk, W. M.; Freedman, T. B.; Nafie, L. A. *Biopolymers* **1989**, *28*, 2025−2044.
(10) Young, D. A.; Freedman, T. B.; Lipp, E. D.; Nafie, L. A. *J. Am. Chem. Soc.* **1986**, *108*, 7255−7263.
(11) Young, D. A.; Freedman, T. B.; Nafie, L. A. *J. Am. Chem. Soc.* **1987**, *109*, 7674−7677.
(12) Paterlini, M. G.; Freedman, T. B.; Nafie, L. A. *J. Am. Chem. Soc.* **1986**, *108*, 1389−1397.
(13) Lal, B. B.; Diem, M.; Polavarapu, P. L.; Oboodi, M.; Freedman, T. B.; Nafie, L. A. *J. Am. Chem. Soc.* **1982**, *104*, 3336−3342.
(14) Nafie, L. A.; Oboodi, M. R.; Freedman, T. B. *J. Am. Chem. Soc.* **1983**, *105*, 7449−7450.
(15) Freedman, T. B.; Nafie, L. A. In *Topics in Stereochemistry*; Eliel, E. L., Wilen, S. H., Eds.; John Wiley & Sons: New York, 1987; Vol. 17, pp 113−206.
(16) Nafie, L. A.; Freedman, T. B. *J. Phys. Chem.* **1986**, *90*, 763−767.
(17) Bursi, R.; Devlin, F. J.; Stephens, P. J. *J. Am. Chem. Soc.* **1990**, *112*, 9430−9432.
(18) Bursi, R.; Stephens, P. J. *J. Phys. Chem.* **1991**, *95*, 6447−6454.
(19) Ashvar, C. S.; Devlin, F. J.; Bak, K. L.; Taylor, P. R.; Stephens, P. J. *J. Phys. Chem.* **1996**, *100*, 9262−9270.
(20) McCann, J.; Rauk, A.; Shustov, G. V.; Wieser, H.; Yang, D. Y. *Appl. Spectrosc.* **1996**, *50*, 630−641.
(21) Ashvar, C. S.; Stephens, P. J.; Eggimann, T.; Wieser, H. *Tetrahedron: Assym.* **1998**, *9*, 1107−1110.
(22) Nafie, L. A. *J. Phys. Chem. A* **1997**, *101*, 7826−7833.
(23) Freedman, T. B.; Gao, X.; Shih, M.-L.; Nafie, L. A. *J. Phys. Chem. A* **1998**, *102*, 3352−3357.
(24) Freedman, T. B.; Shih, M.; Lee, E.; Nafie, L. A. *J. Am. Chem. Soc.* **1997**, *119*, 10620−10626.
(25) Nafie, L. A.; Freedman, T. B. *J. Chem. Phys.* **1983**, *78*, 7108−7116.
(26) Yang, D.; Rauk, A. *J. Chem. Phys.* **1992**, *97*, 6517−6534.
(27) Yang, D.; Rauk, A. In *Reviews in Computational Chemistry*; Lipkowitz, K. B., Boyd, D. B., Eds.; VCH Publishers: New York, 1996; Vol. 7, pp 261−301.
(28) Sugeta, H.; Marcott, C.; Faulkner, T. R.; Overend, J.; Moscowitz, A. *Chem. Phys. Lett.* **1976**, *40*, 397−398.
(29) Su, C. N.; Keiderling, T. A. *J. Am. Chem. Soc.* **1980**, *102*, 511−515.
(30) Nakao, Y.; Sugeta, H.; Kyogoku, Y. *Chem. Lett.* **1984**, 623−626.
(31) Diem, M.; Gotkin, P. J.; Kupfer, J. M.; Tindall, A. G.; Nafie, L. A. *J. Am. Chem. Soc.* **1977**, *99*, 8103−8104.
(32) Diem, M.; Photos, E.; Khouri, H.; Nafie, L. A. *J. Am. Chem. Soc.* **1979**, *101*, 6829−6837.
(33) Diem, M.; Gotkin, P. J.; Kupfer, J. M.; Tindall, A. G.; Nafie, L. A. *J. Am. Chem. Soc.* **1978**, *100*, 5644−5650.
(34) Freedman, T. B.; Cianciosi, S. J.; Ragunathan, N.; Baldwin, J. E.; Nafie, L. A. *J. Am. Chem. Soc.* **1991**, *113*, 8298−8305.
(35) Long, F.; Freedman, T. B.; Tague, T. J.; Nafie, L. A. *Appl. Spectrosc.* **1997**, *51*, 508−511.
(36) Long, F.; Freedman, T. B.; Hapanowicz, R.; Nafie, L. A. *Appl. Spectrosc.* **1997**, *51*, 504−507.
(37) Frisch, M. J.; Trucks, G. W.; Schlegel, H. B.; Gill, P. M. W.; Johnson, B. G.; Robb, M. A.; Cheeseman, J. R.; Keith, T.; Petersson, G. A.; Montgomery, J. A.; Raghavachari, K.; Al-Laham, M. A.; Zakrzewski, V. G.; Ortiz, J. V.; Foresman, J. B.; Peng, C. Y.; Ayala, P. Y.; Chen, W.; Wong, M. W.; Andres, J. L.; Replogle, E. S.; Gomperts, R.; Martin, R. L.; Fox, D. J.; Binkley, J. S.; Defrees, D. J.; Baker, J.; Stewart, J. P.; Head-Gordon, M.; Gonzalez, C.; Pople, J. A. *Gaussian 94*; B.3 ed.; Gaussian, Inc.: Pittsburgh, PA, 1995.
(38) Rauk, A.; Yang, D. *J. Phys. Chem.* **1992**, *96*, 437−446.
(39) Eggimann, T.; Shaw, R. A.; Wieser, H. *J. Phys. Chem.* **1991**, *95*, 591−598.
(40) Frisch, M. J.; Head-Gordon, M.; Trucks, G. W.; Foresman, J. B.; Schlegel, H. B.; Raghavachari, K.; Robb, M. A.; Brinkley, J. S.; Gonzalez, C.; Defrees, D. J.; Fox, D. J.; Whiteside, R. A.; Seeger, R.; Martin, L. R.; Baker, J.; Kahn, L. R.; Stewart, J. J. P.; Topiol, S.; Pople, J. A. *Gaussian 90*; Gaussian Inc.: Pittsburgh, PA, 1990.
(41) Gigante, D. M. P. Ph.D. Dissertation, Syracuse University, Syracuse, NY, 1993.
(42) Lavalley, J. C.; Sheppard, N. *Spectrochim. Acta* **1972**, *28A*, 2091−2101.
(43) Keiderling, T. A.; Stephens, P. J. *J. Am. Chem. Soc.* **1977**, *99*, 8061−8062.
(44) Marcott, C.; Blackburn, C. C.; Faulkner, T. R.; Moscowitz, A.; Overend, J. *J. Am. Chem. Soc.* **1978**, *100*, 5262−5264.
(45) Wood, R. L. M.S. Thesis, Syracuse University, Syracuse, NY, 1989.
(46) Dybal, J.; Krimm, S. *J. Mol. Struct.* **1988**, *189*, 383−392.
(47) Ribeiro-Claro, P. J. A.; Teixeira-Dias, J. J. C. *J. Raman Spectrosc.* **1984**, *15*, 224−231.
(48) Polavarapu, P. L.; Ewig, C. S.; Chandramouly, T. *J. Am. Chem. Soc.* **1987**, *109*, 7382−7386.
(49) Su, C. N. Ph.D. Dissertation, University of Illinois, Chicago Circle, IL, 1980.
(50) Freedman, T. B.; Lee, E.; Nafie, L. A. Submitted for publication.